

Document downloaded from:

<http://hdl.handle.net/10251/194926>

This paper must be cited as:

Ordóñez, R.; Atarés Huerta, LM.; Chiralt Boix, MA. (2022). Antilisterial action of PLA films with ferulic acid as affected by the method of incorporation. Food Bioscience. 49:1-11. <https://doi.org/10.1016/j.fbio.2022.101865>



The final publication is available at

<https://doi.org/10.1016/j.fbio.2022.101865>

Copyright Elsevier

Additional Information

1 **Antilisterial action of PLA films with ferulic acid as affected by the method of**
2 **incorporation.**

3 Ramón Ordoñez ^{a,1,*}, Lorena Atarés^{a,2}, Amparo Chiralt ^{a,3}

4 ^aInstituto Universitario de Ingeniería de Alimentos para el Desarrollo.

5 Universitat Politècnica de València, Camino de Vera, s/n, 46022 Valencia, Spain.

6 ¹raorla@doctor.upv.es ²loathue@tal.upv.es ³dchiralt@tal.upv.es

7

8 Abstract

9 Previous studies demonstrated that polylactic acid (PLA) films with ferulic acid (F) obtained by melt blending
10 did not release the active compound to exert effective antibacterial action. To solve this problem, different
11 strategies to promote the active properties of PLA-F materials have been studied: film processing by casting
12 with F up to 10 w/w, surface loading of thermoprocessed films with F, by adsorption or pulverisation with F
13 solutions, and electrospinning of PLA-F solutions, using different solvent systems, to obtain nanostructured
14 mats. The materials obtained were characterised by their morphological properties and antilisterial activity.
15 F crystallised inside cast films and on the surface loaded PLA films. Electrospun materials exhibited different
16 morphology, depending on the solvent system of the initial solution; fibre mats were obtained with ethyl
17 acetate-DMSO mixtures, whereas bead structures were mainly formed with glacial acetic acid with or without
18 ethyl acetate. No antilisterial activity was observed in cast films regardless of the F concentration, whereas
19 surface loaded films by adsorption or pulverisation inhibited the listeria growth by about 4 Log(CFU/mL).
20 Electrospun materials only inhibited bacterial growth (3 Log CFU) when these were fibre-structured.
21 Therefore, active films of PLA with F could be only obtained when the active was surface anchored or
22 encapsulated in thin fibre mats, with high surface to volume ratio. In this way, the release of the active
23 compound is promoted, avoiding the problem of its limited internal diffusion through the PLA matrix.

24

25 **Keywords:** PLA, antimicrobial, electrospinning, pulverisation, ferulic acid, active food packaging.

26 Highlights

27 Alternative methods to incorporate ferulic acid (F) into a PLA matrix were studied

28 No bacterial inhibition was observed for cast PLA films with different concentrations of F

29 Film surface anchoring of F by adsorption or pulverisation provoked bacteriostatic effect

30 Fibre or bead formation in electrospun PLA-F materials depended on the used solvent

31 Fibre structured electrospun materials inhibited bacterial growth, unlike those bead-structured

32

33 1. Introduction

34 As the global environmental crisis escalates due to the uncontrolled use of petroleum-based plastics, the
35 food packaging industry needs alternative solutions capable of ensuring food quality and safety while driving
36 the operations to more sustainable practices. These practices also include the reduction of chemical
37 additives used for food preservation; hence, there is growing interest in the use of naturally occurring
38 compounds with antimicrobial and antioxidant properties (Atarés & Chiralt, 2016). Polylactic acid (PLA) is a
39 widely studied biodegradable polymer obtained by synthesis from lactic acid coming from the fermentation
40 of biomass sources (Armentano et al., 2013). It exhibits good properties for food packaging purposes
41 (Velásquez et al., 2021; Muller et al., 2017a) and it is considered to be the most promising bioplastic, based
42 on its production and the growing tendency on patents filings (Elvers et al., 2016). The beneficial properties
43 of PLA include good mechanical strength and thermoforming ability, biocompatibility, composting ability and
44 monomer renewability, although its inherent brittleness and low thermal resistance limit some of its
45 packaging applications. Its functional properties can be improved by incorporating bioactive compounds into
46 the polymer matrix, which can contribute to the enhancement of its ability for food preservation and shelf-life
47 extension, thus adding value to the material and increasing its competitiveness in the packaging market. Of
48 the naturally occurring bioactive compounds, ferulic acid (F) is a hydroxycinnamic acid, commonly present
49 in a great variety of plant species, which exhibit antimicrobial (Miyague et al., 2015; Pernin et al., 2019; Shi
50 et al., 2016) and antioxidant properties (Itagaki et al., 2009; Rice-Evans et al., 1996; Zduńska et al., 2018).
51 It has low toxicity and possesses many physiological functions (anti-inflammatory, antioxidant, antimicrobial
52 activity, anticancer, and antidiabetic effect), being widely used in the pharmaceutical, food, and cosmetics
53 industry (Paiva et al., 2013).

54 Incorporation of active compounds, such as F, into biodegradable polymers, such as PLA, could result in
55 active and biodegradable packaging materials useful to extend food shelf life (Muller, et al., 2017b), with
56 better environmental performance than conventionally used plastics (Lorite et al., 2017). In a previous study,
57 F has been incorporated into PLA matrices, by using melt-blending and compression moulding to obtain
58 potentially active films (Ordoñez et al., 2022). However, the resulting materials did not exhibit significant
59 antimicrobial activity, which was attributed to the limited release of the active compound due to the low
60 molecular mobility in the glassy polymeric matrix ($T_g \approx 55^\circ\text{C}$) that inhibits diffusion processes (Chung & Kwak,

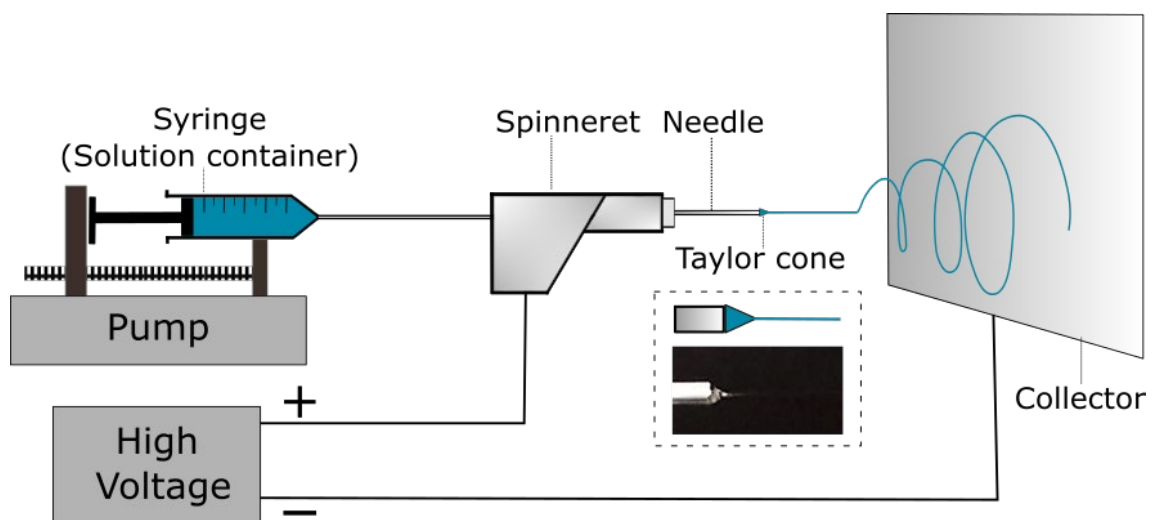
61 2019). In this sense, alternative methods to incorporate F into the PLA matrix that would favour its
62 antimicrobial action are of great interest, given the marked potential of these films for food preservation
63 purposes. To this aim, two possibilities can be envisaged: a) promotion of the internal diffusion of the active
64 compound through the polymer matrix (e.g. by plasticising) and b) anchoring the compound on the film
65 surface to avoid the hindered internal mass transfer through the film. Likewise, encapsulation of the active
66 compound in nanostructured materials, with high surface-volume ratio, could also favour its release and
67 antimicrobial action.

68 To obtain more plasticized PLA films, solvent casting could be used. It consists of formulating polymeric
69 solutions, where additives (plasticisers, active components...) can be incorporated, and later allowing the
70 solvent to evaporate in order to form the film (Suhag et al., 2020). In polymeric films obtained by casting,
71 residual solvent retention generally occurs due to the solvent-polymer interactions that hinder the complete
72 evaporation of the solvent. The retained solvent acts as a plasticizer in the polymer matrix, giving rise to
73 more plasticized films (lower T_g), with higher molecular mobility (Ordoñez et al. 2022; Muller et al., 2017b).
74 This can enhance the release of incorporated active compounds from the matrix, compared to those polymer
75 matrices obtained by thermal processing. The coating of thermo-processed PLA films with a thin layer of F-
76 loaded PLA solution could be used to obtain active films, facilitating the release of the active in contact with
77 the food substrate.

78 Different methods could be used to produce surface loaded PLA films with F, such as the compound
79 adsorption on the film from a concentrated F solution or the film spraying with a F solution. In this sense,
80 previous studies reported good adsorption of ferulic acid on Amberlite XAD16 from organic waste effluents
81 (Dávila-Guzman et al., 2012). The driving force of the adsorption phenomena is the compound chemical
82 potential that increase with the compound concentration in the solution. Adsorption mechanisms and the
83 yield of the process are affected by a wide number of factors, such as the relative chemical affinity between
84 the compound and the surface and the solvent, temperature or pH (Dávila-Guzman et al., 2012; Pholosi et
85 al., 2020). Thus, the superficial anchoring of the ferulic acid on the PLA film surface could be achieved by
86 the film's immersion in a concentrated solution of the acid. Likewise, the pulverisation of a F solution on the
87 film surface, using a flow controlled device, can also be used to produce ferulic surface-loaded PLA films,
88 using a volatile solvent to favour the evaporation process and compound deposition (Main et al., 1978).

89 Electrospinning is an alternative process to produce F delivery systems from PLA. This technique makes it
90 possible to obtain nanostructured materials, with high specific area, which may be deposited on the film
91 surface to promote the compound release. It consists of propelling a stream of a polymeric solution when
92 submitted to an electrical field that accelerates and spins the stream while evaporating most of the solvent.
93 As a result, the polymeric material is deposited on a collector plate (Wang & Ryan, 2011). **Figure 1** shows
94 a basic electrospinning setup. The electrospinning process gives rise to the deposition of polymer fibres,
95 which are elongated strands of polymer with high surface to volume ratio. If the jet is interrupted, depending
96 on the process conditions, electrospaying rather than electrospinning occurs, giving rise to the formation of
97 polymer beads (round or oval structures with lower surface to volume ratio than the fibres).

98



99

100 **Figure 1** Basic electrospinning setup with main components and Taylor cone illustration.

101 In previous studies, electrospinning has been used to incorporate active compounds into **PLA matrices**, in
102 **order to develop active materials for food packaging**. To this end, **polymeric solutions with active compounds**
103 **were used to produce their encapsulation in the electrospun material (mats) after solvent evaporation under**
104 **the electric field (Tampau et al., 2020)**. The **electrospun mats** present a high surface area that enhances the
105 release of active compounds into the food matrices or simulants (Alonso-González et al., 2020). The
106 properties of the polymeric solutions, such as surface tension, electrical conductivity or viscosity, determine
107 the stability of the operation and the viability of the electrospinning process. A stable cone formation of the
108 stream at the tip of the needle, known as the Taylor cone, is considered as an indicator of steady-state
109 process (Bhattacharjee & Rutledge, 2017). In order to reach operational stability, a number of variables must
110 be controlled, both related to the solution properties (solvent volatility, conductivity, viscosity or surface
111 tension) and the process conditions, such as flow rate, electric potential applied and needle-collector
112 distance (Castro Coelho et al., 2021). Tampau et al. (2020) studied the combination of several solvents to
113 obtain electrospun fibres of PLA, and found that volatile solvents, such as ethyl acetate (E), needed to be
114 combined with other less volatile solvents, such as DMSO (D) or acetic acid (A), to achieve a stable
115 electrospinning operation.

116 In this study, four kinds of PLA materials loaded with ferulic acid, with potential antibacterial properties, were
117 produced for food packaging applications. These were: a) cast films from ethyl acetate polymeric solutions
118 with different concentration of F, b) F-surface loaded thermoprocessed PLA films by adsorption from
119 concentrated solutions of the active compound, c) F-surface loaded thermoprocessed PLA films by
120 pulverisation with a concentrated F solution and d) electrospun PLA-F materials using PLA-F solutions with
121 different solvent systems. The final content of ferulic acid, as well as the morphological and antilisterial
122 properties of the different materials were analysed.

123

124 **2. Materials and methods**

125 **2.1. Materials**

126 Amorphous PLA 4060D (106 kDa MW, Nature Works, MN, USA) and ferulic acid (Sigma-Aldrich, St. Louis,
127 USA) were used to formulate active films. Ethyl acetate (Indukern, Barcelona, Spain), dimethyl sulfoxide
128 (DMSO), glacial acetic acid, methanol and ethanol 96% (obtained from Panreac Química, Barcelona, Spain)
129 were used as solvents. Tryptone soy broth (TSB), bacteriological agar, peptone water and Palcam agar base
130 (PAB) enriched with palcam selective supplement for *Listeria* were obtained from Scharlab (Barcelona,
131 Spain) and used for antibacterial tests. The bacterial strain, *Listeria innocua* (CECT 910), was supplied by
132 the Spanish Type Collection (CECT, University of Valencia, Spain).

133 **2.2. Methods**

134 **2.2.1 Production of cast PLA films with ferulic acid**

135 PLA films with incorporated F (0%-10% w/w in the film) were obtained by casting **as described by Muller, et**
136 **al. (2017b)**. **Film-forming solutions with 10% w/w solids were obtained in ethyl acetate by dissolving PLA**
137 **and F at different proportions (2, 3, 4, 5, 7 and 10 g F/100 g solids)**. The different solutions (40 g) were
138 poured onto 15 cm diameter Teflon levelled plates and left to dry overnight, **at room temperature (20 °C)**.
139 **Afterwards, the films, with about 250 µm in thickness, were peeled from the plate.**

140 **2.2.2. Production of thermoprocessed PLA films**

141 Pure PLA films were also obtained by **thermoccompression** moulding using a heat plates hydraulic press
142 (LP20, Labtech Engineering, Thailand). Ground and dried PLA pellets (4 g) were placed into 15 cm circular
143 Teflon moulds in the press. An initial preheating step was applied for 4 min at 200 °C followed by a
144 compression step at 10 MPa and the same temperature for 4 min; finally, a cooling step lowered the
145 temperature to 70 °C in 3 min. **Films of about 200 µm in thickness were obtained.**

146 **2.2.3. Adsorption of ferulic acid on the thermoprocessed PLA films**

147 F was adsorbed on the surface of **thermoprocessed** PLA films by immersion in three different F-saturated
148 solution systems, namely distilled water (0.1% w/w F), ethanol 10% v/v (0.1% w/w F) and ethanol 96% v/v
149 (11.2% w/w F). Film strips (1 x 4.5 cm and 1± 0.1 g) were immersed in the solutions and kept under magnetic
150 stirring at 150 rpm and 25 °C. The maximum immersion time was 96 h for water and 10% ethanol, and only
151 4 h for 96% ethanol, due to film deformation. The samples were removed from the F solutions at different
152 times, drained for 1 min and vacuum (0.1 atm) dried at 60 °C for 24-36 h until reaching constant weight. The
153 F content was determined spectrophotometrically (UV-visible spectrophotometer Thermoscientific Evolution
154 201, USA) after the methanolic extraction of dry films. To this end, the samples were immersed in 10 mL

155 methanol and kept under magnetic stirring at room temperature (20 °C) for 72 h. The absorbance
156 measurements at 320nm were carried out after filtration and proper dilution. A previously determined F-
157 methanol calibration curve was used to quantify the F adsorbed on the film surface, and the results were
158 expressed as mg F/ g treated film. To determine the real superficial anchoring of F, some samples were
159 washed in their corresponding solvent before F was quantified and the resulting amounts were compared.

160 To study the F adsorption kinetics, the experimental results were fitted to the Peleg model (Peleg, 1988)
161 (Eq. 1).

$$162 \quad M(t) = M_0 + \frac{t}{k_1 + k_2 \cdot t} \quad (\text{Eq. 1})$$

163 Where: M(t) is the mass of ferulic acid incorporated per mass unit of film at a given time (mg/g); M₀ is the
164 initial mass of F per mass unit of film (0 mg/g); t is the adsorption time (h); k₁ and k₂ are model constants: k₁
165 is inversely related to the release rate (1 / k₁), while k₂ is inversely related to the asymptotic adsorption value
166 (M_∞= 1/k₂).

167 A second batch of samples was prepared to evaluate the antimicrobial effect of PLA films with adsorbed F.
168 To this end, circular film samples (5.5 cm diameter) to cover the Petri dishes, were immersed in the 11.2%
169 F solution (solvent ethanol 96% v/v) for 30 min to reach a determined load of F, according to the kinetic
170 analyses.

171 **2.2.4. Pulverisation of ferulic acid solutions on the thermoprocessed PLA films**

172 Thermoprocessed PLA films were surface loaded by pulverisation of F solution on the film surface. Ethanol
173 was selected as the solvent for pulverisation due to its volatility and the high solubility of F. A saturated
174 solution of F in 96% (v/v) ethanol (11.2 g of F per 100 g of solution) was filtered and loaded in an airbrush
175 (E4182, Elite pro) container equipped with a 0.8 mm nozzle. The solution was sprayed on circular 5.5 cm
176 diameter PLA films for 5 seconds, at 7.83 mL/s airbrush flow. The pulverised film samples were vacuum
177 dried at 60 °C and 0.1 atm for 24-36 hours until reaching constant weight. The loaded amount of F on the
178 film surface was quantified gravimetrically.

179 **2.2.5. Production of electrospun PLA-F materials**

180 PLA materials loaded with F were also obtained by electrospinning. To this end, 15% w/w PLA solutions
181 with 15% w/w F with respect to total solids, were prepared. The PLA pellets were placed in the selected
182 solvent systems in hermetically sealed recipients and maintained under magnetic stirring at room
183 temperature (25 ± 1 °C) for 24 h to ensure complete dissolution, afterwards incorporating F. The selection
184 of the solvents was carried out by considering the adequate solubility of the polymer and the active
185 compound, their food contact properties and the adequate response of the solution to the electric field (stable
186 Taylor cone and jet formation). Based on these requirements, DMSO (D), ethyl acetate (E) and glacial acetic
187 acid (A) were selected and some of their mixtures were tested, based on previous studies (Tampau et al.,
188 2020). Ethyl acetate (E) is a good solvent for amorphous PLA, but its high degree of volatility (boiling point:
189 77 °C) prevents a steady electrospinning stream. Therefore, blends of E with less-volatile solvents were
190 used. E was mixed with DMSO (D, boiling point: 189 °C) in two volumetric ratios 1:1 and 3:2 (E:D). Acetic
191 acid (A, boiling point: 118 °C) was used both pure and in a 1:1 volume mixture with E. Hence, the polymeric
192 solutions of PLA and F were referred according to the solvent system used: ED1:1, ED3:2, EA1:1, and A1.

193 **Process conditions**

194 The electrospinning operation was carried out in Fluidnatek LE-10 (Bioinicia SA, Valencia, Spain) equipment,
195 using single flow monoaxial mode at 25±1 °C and 45% RH. 5 mL disposable syringes (BD Plastik) were
196 used to load the solutions into a PTFE tube connected to the spinneret with a 0.6 mm stainless-steel needle.
197 The stream was deposited on a stainless-steel collector covered with previously weighed aluminium foil.
198 Both needle and collector were connected to a high voltage source (0-30 kV). Relevant operation
199 parameters, such as flow rate, voltage and injector-collector distance, were adjusted empirically aiming for
200 the formation of a stable Taylor cone in the tip of the spinneret (Tampau et al., 2020). The operation time in
201 samples used for antimicrobial analyses was adjusted for each formulation in order to obtain a mass of mats
202 containing the target amount of ferulic acid. This target was defined as the amount of F necessary to reach
203 the minimal inhibitory concentration of the bacteria in the culture plate when coated with the obtained mat,
204 assuming a total release on the loaded F. The materials obtained were stored in desiccators with silica gel
205 at room temperature until their use.

206 **Characterization of PLA-ferulic acid solutions**

207 The relevant properties for the electrospinning process of the PLA-F solutions with the different solvents
208 were characterised.

209 Density was determined, at 20 °C, in duplicate, with an immersion densimeter (Alla France).

210 **Electrical** conductivity was measured twice per formulation using a Mettler Toledo (Switzerland) SevenEasy
211 conductometer, at 20 °C.

212 Surface tension was assessed by the pendant drop method with an OCA 20 instrument (Dataphysics,
213 Germany) using software SCA 20, performing 9 repetitions per formulation, at 25 °C.

214 Rheological behaviour, at 25 °C, was measured in triplicate per formulation, using a rheometer (HAAKE
215 Rheostress 1, Thermo Electric Corporation, Germany) with a coaxial cylinder system (Z34DIN Ti), between
216 0 and 600 s⁻¹.

217 **Encapsulation efficiency of ferulic acid**

218 The content of ferulic acid in the mats was determined by methanolic extraction and UV-visible
219 spectrophotometry, as described above. The encapsulation efficiency was determined as the ratio between
220 the quantified amount of F, per mass unit of polymer in the mat, with respect to the used proportion in the
221 initial solution (0.176 g F/g PLA).

222 **2.2.6. Microstructural observations**

223 The materials obtained were observed using a field emission scanning electronic microscope (FESEM, Ultra
224 55, Zeiss, UK) at an acceleration voltage of 2 kV. The surface observations were carried out for all materials
225 while images of the film cross-section were taken for materials obtained by adsorption and pulverisation.
226 The images were obtained at 100x and 400x magnification level. Before observation, samples were
227 cryofractured by immersion in liquid nitrogen (only for cross-section observations), mounted on sample
228 holders with carbon tape and platinum coated (one coat). ImageJ software (v.153c, National Institute of
229 Health, Bethesda, USA) was used to measure the diameter of beads and fibres in the electrospun mats (60
230 measured elements per sample).

231 **2.2.7. Antibacterial activity assessment**

232 *In vitro* antibacterial activity with *Listeria innocua* was performed according to previous studies (Ordoñez et
233 al., 2021; Tampau et al., 2018). All materials, devices and previously prepared media were sterilised with
234 UV-light inside a laminar flow cabinet (Bio II advance, Telstar, Spain). 10 mL of TSA were poured into 55
235 mm Petri dishes and inoculated with 100 µL of *L. innocua* bacterial suspension (10⁵ CFU / mL) on the plate
236 surface using a L-form rod, aiming for an initial concentration of 10³ CFU / mL. The TSA was covered with
237 films from the obtained materials; the Petri dishes were sealed with Parafilm™ and left to incubate at 10 °C
238 for 6 days. After this time, the TSA and samples were homogenised in 100 mL of buffered peptone water for
239 2 min, employing a masticator paddle blender (IUL Instruments, Barcelona, Spain). The serial dilutions were
240 plated and covered with Palcam Agar base previously enriched with *Listeria* selective supplement. After 48
241 hours at 37 °C incubation, the colonies were counted. Each material was tested in triplicate and all the
242 dilutions were plated and counted in duplicate.

243 **2.3. Statistical analysis**

244 Data statistics were evaluated through analysis of variance (ANOVA) using Statgraphics Centurion XVIII
245 software (Statgraphics Technologies, Inc. The Plains, Virginia). Fisher's least significant difference was used
246 at a 95% confidence level, different superscripts in tables ^(abc) indicate significant differences.

247 **3. Results and discussion**

248 **3.1. Cast PLA films containing ferulic acid**

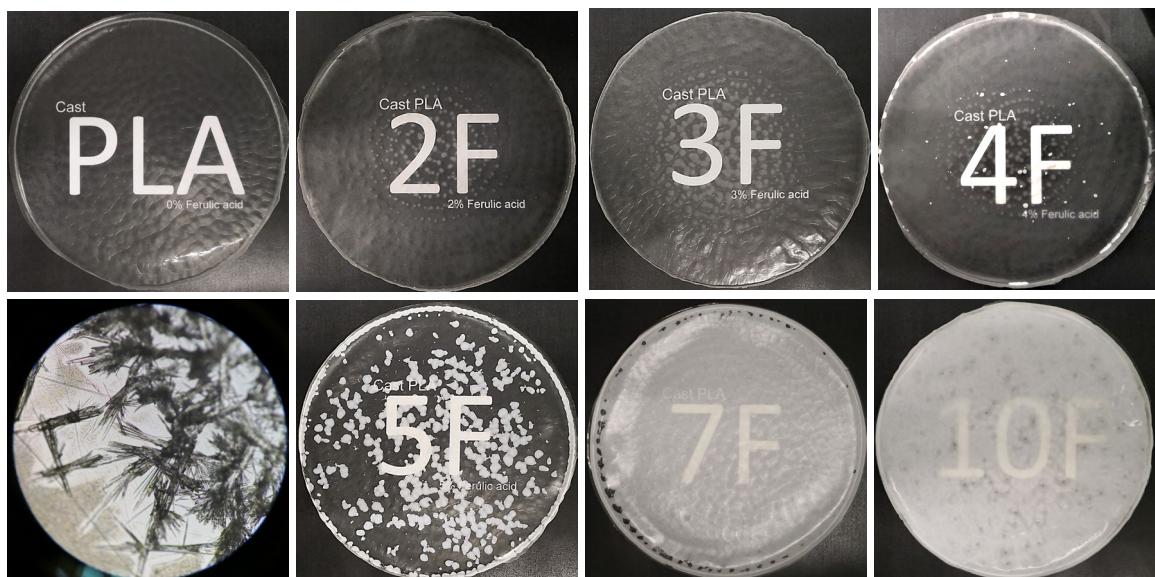
249 **Figure 2** shows images of the PLA and PLA-F films (2%-10% F in the film) obtained by casting. All the
250 formulations with F presented crystalline formations, which were visible to the naked eye. **Figure 2** also
251 shows an optical microscope image of the F crystals in the cast films. These crystals exhibited similar
252 morphology to those observed by other authors (Paiva et al., 2013; Chen et al. 2020) for ferulic acid trans
253 isomer that tends to crystallise forming prolonged white crystalline aggregates. This crystallization can be
254 explained considering solubility of F in ethyl acetate and thermodynamic compatibility of both solutes (PLA
255 and F) in the solvent. Solubility of ferulic acid in ethyl acetate, as reported by Shakeel et al. (2017), is
256 1.98×10⁻² in mol fraction, at 318.2 K. This concentration would be achieved in the solvent when this
257 evaporates during the film formation. When saturation is reached, crystallisation of F could occur, but this

258 process would be interfered by the polymer-F interactions and solute-solvent interactions, depending on the
259 thermodynamic compatibility of both solutes. Moreover, crystal growth will be affected by the solution
260 viscosity that increases during solvent evaporation. In fact, no visual crystals were observed in
261 thermoprocessed films of PLA with ferulic acid (Ordoñez et al., 2022), which could be attributed to the high
262 viscosity of the melt that inhibits the crystal growth. Both compounds formed homogenous solutions in ethyl
263 acetate at the used concentrations, but when saturation of F is reached due to the solvent evaporation, it
264 crystallises. Ferulic acid crystallisation demonstrates its thermodynamic incompatibility with PLA. Crystal
265 growth was enhanced due to the lower viscosity of the PLA solutions as compared with the PLA melt.

266 Despite the inadequacy of these materials for packaging purposes, they were proven to exert antibacterial
267 activity, since they contain growing amounts of active compound that could be released into the culture
268 media to differing extents, giving rise to varying levels of bacterial growth inhibition.

269

270



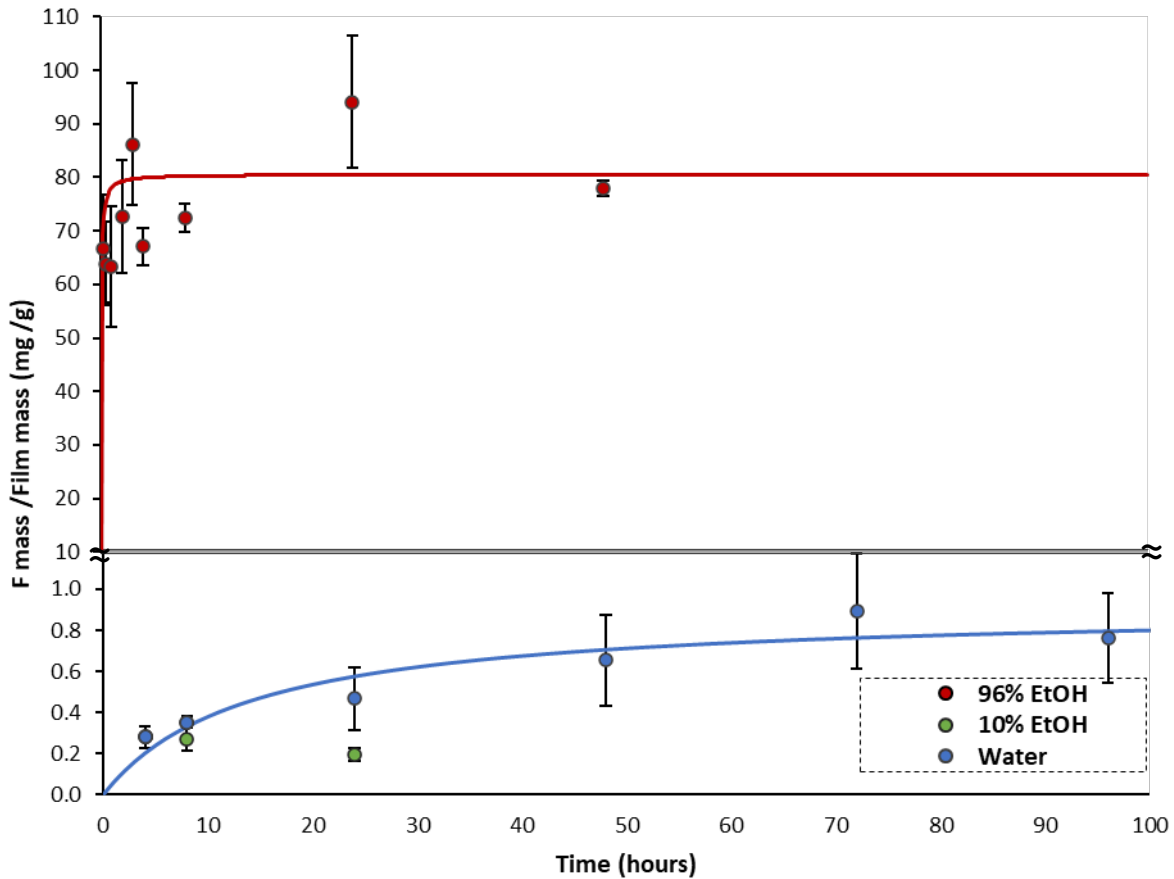
271 **Figure 2:** Cast PLA and PLA-F films (2%-10% w/w F in the film). The bottom left picture shows crystalline
272 formations of ferulic acid in the films as observed through an optical microscope (10X).

273 **3.2. Thermoprocessed PLA films with adsorbed ferulic acid**

274 Ferulic acid surface adsorption was successfully achieved, and F crystals were formed on the surface of the
275 film samples immersed in all three F solutions, both with and without washing the films with their
276 corresponding solvent. **Figure 3** shows the experimental values of F adsorbed on the PLA surface (mg F/g
277 film) as a function of the immersion time. The low solubility of F in water, **due to its limited capacity to form**
278 **hydrogen bonds** (Mota et al., 2008), and the subsequent low concentration of F in the saturated solution,
279 limited the adsorption of the acid molecules on the PLA films from the aqueous systems. In the 10% ethanol
280 solution, only 0.27 mg F/g film were adsorbed after 24 h immersion, **with no significant increase throughout**
281 **time, despite the similar mass fraction of F determined in water and 10% ethanol saturated solutions (~0.1%**
282 **w/w, at room temperature)**. The lower adsorption of F when using 10% ethanol can be due to the change in
283 the balance of interaction forces of compound-solvent and compound-PLA surface. The chemical affinity of
284 F with ethanol solution is greater than that with water, and interactions with PLA could also change due to
285 the structural modifications that ethanol provokes in the PLA matrix (swelling and matrix relaxation), as
286 reported by other authors (Jamshidian et al., 2012). **On the basis of these results, the 10% ethanolic system**
287 **was excluded from further study**. In pure water, a small but steady increase in the F adsorbed on the films
288 was achieved, this being 0.76 mg/g after 96 hours. On the other hand, the samples immersed in 96% ethanol,
289 with 11.2% F, presented remarkably higher values of adsorbed F, reaching 63 mg/g after an immersion of
290 only 15 min. The highest concentration of F in the solution implied this compound had a high gradient of
291 chemical potential between the solution and the film surface, hence representing a great driving force for the
292 adsorption process. However, after 4 hours of immersion, the film strips started to deform, which was
293 attributed to the ethanol diffusion into the matrix, promoting polymer relaxation and swelling and even partial
294 degradation, as reported by other authors in the case of the PLA films in contact with ethanol rich aqueous
295 solvents (Jamshidian et al., 2012).

296 To assess the real anchoring of ferulic acid on the surface of the films, a set of samples was washed with
 297 the corresponding solvent after the adsorption process. While the samples immersed in water lost about
 298 84% of F by washing, those immersed in 96% ethanol only lost 55% of the initially retained acid. Apart from
 299 confirming the differences between the adsorption media used, this result suggests that most of the F
 300 molecules are attached to the film's surface by weak interactions (hydrophobic interactions and hydrogen
 301 bonds), thus allowing an effortless release. When using 96% ethanol, more internal diffusion of F from the
 302 PLA surface could occur, due to the swelling and relaxation of the polymer matrix in contact with the solvent,
 303 which promotes diffusion-controlled mass transfer into the film. Thus, the more internally located F molecules
 304 were not dragged by the washing solvent.

305



306 **Figure 3** Adsorbed amounts (mean values and standard deviation) of ferulic acid (mg/g film) on the PLA
 307 films, as a function of time, with the different solution systems (distilled water with 0.1% F, 10% v/v ethanol
 308 with 0.1% F and 96% v/v ethanol with 11.2% F). The continuous lines represent the fitted Peleg model.

309 The Peleg equation was used to model the adsorption kinetics of F from both water and 96% ethanol
 310 solutions and to determine the immersion time needed to prepare samples for the antimicrobial tests with a
 311 determined F load. The resulting parameters are shown in **Table 1** and the corresponding predictions are
 312 represented in **Figure 3**.

313 **Table 1** The Peleg model's kinetic parameters for ferulic acid adsorption on PLA films during immersion in
 314 F saturated solutions in water and 96% ethanol.

Parameter	Water	96% Ethanol
k_1 ($h \cdot g \cdot mg^{-1}$)	15.4	$4 \cdot 10^{-4}$
k_2 (g/mg)	1.09	0.012
M_{∞} (mg/g)	0.912	80.6
R^2	0.956	0.992

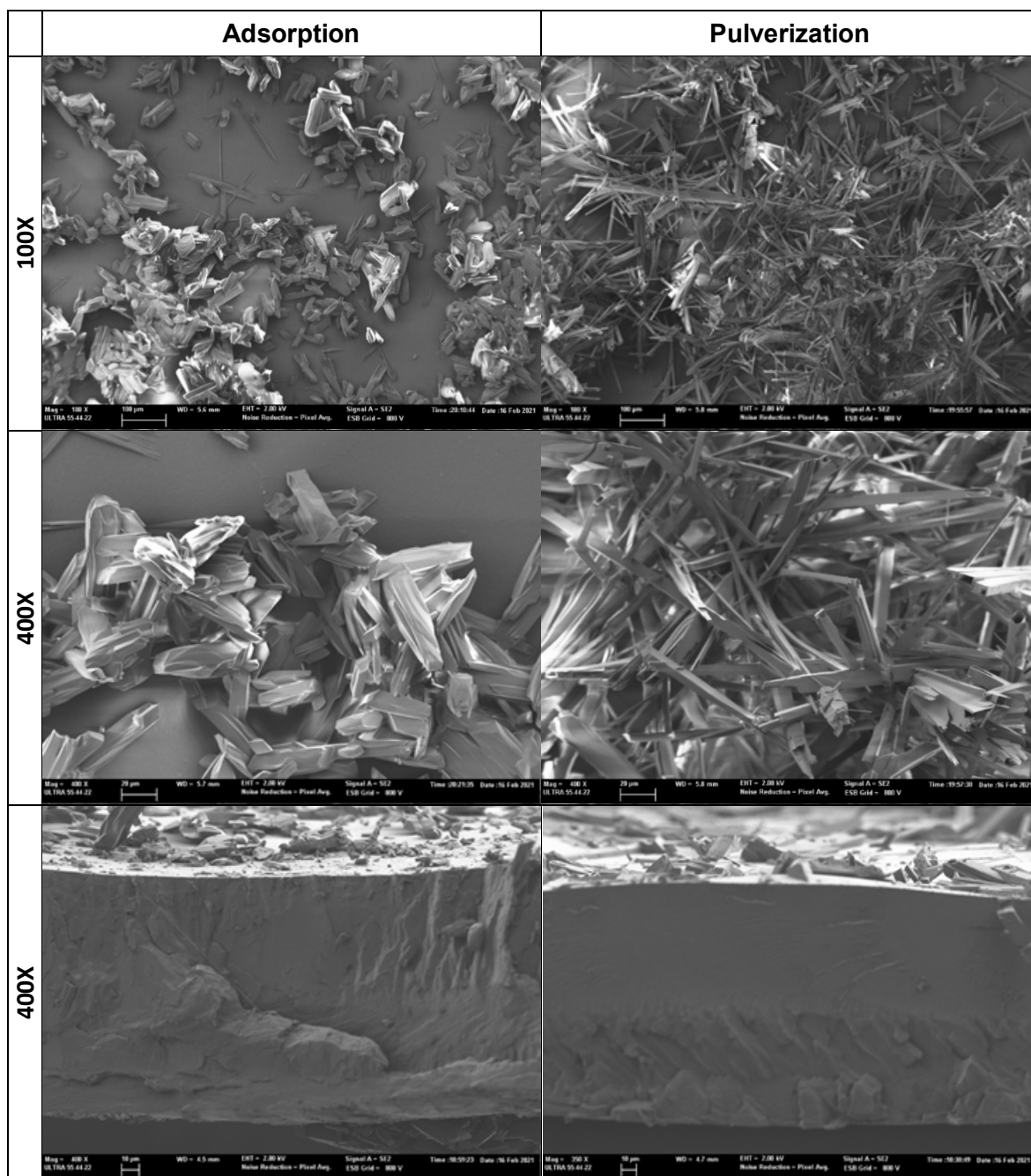
315

316 Despite the highly variable nature of the experimental data, which could be attributed to a heterogenous film
317 drainage, the high values of R^2 demonstrate the good fit of the Peleg model. Given the high adsorption rate
318 of F in the 96% ethanolic system, k_1 (inversely related to the process rate) was a great deal lower for this
319 series. The resulting asymptotic values of F adsorption (M_∞) are inversely related to k_2 . Coherently with the
320 experimental data, M_∞ was two orders of magnitude higher for the 96% ethanolic system than for the water
321 system. Reaching 90% of M_∞ took 72 h for the samples immersed in the water, while only 8 h were necessary
322 in the 96% ethanol. Due to the small amount of F adsorbed from the aqueous solution, these samples were
323 discarded for both antimicrobial testing and further characterisation. For the samples immersed in the 96%
324 ethanol, an immersion time of 30 min (when 66% of M_∞ had been reached) was fixed to prepare film samples
325 destined for antibacterial tests, reaching a compromise between the adsorption of F on the film surface and
326 the lower degree of film deformation.

327 **3.3. Thermoprocessed PLA films with pulverised ferulic acid**

328 Spraying PLA films with ethanolic ferulic acid solution (11.2% w/w) led to the formation of a uniform layer of
329 firmly adhered F crystals when dried. This method was more effective than adsorption at loading PLA films,
330 since the incorporation of F reached 10% w/w F in the film, while consuming less solvent and time. FESEM
331 observations were carried out to compare the microstructure of the ferulic-loaded film surface obtained by
332 ethanolic adsorption and pulverisation, with F crystalline formations (**Figure 4**). **The needle-like morphology**
333 **of the crystals, as reported by Chen et al. (2020) for ferulic acid agglomerates, was observed in both cases.**
334 **Nevertheless,** crystalline formations in the adsorption films were broader and shorter than those obtained by
335 pulverisation, which could be related to the different crystallisation kinetics and internal diffusion of F
336 molecules that occurred in each case, with different process times. **Crystallisation of F on the surface of**
337 **pulverised films points to a very limited internal diffusion of F into PLA matrix during the process. In fact,**
338 **FESEM images of the cross-section of the films (Figure 4) did not reveal the internal diffusion of F, but its**
339 **accumulation as crystals on the surface due to the fast evaporation of the ethanol. Diffusion times are longer**
340 **than solvent evaporation times and so, the solute separates from the solvent as adhered crystals on the film**
341 **surface. Therefore, most of the F anchoring occurred on the film surface as crystalline formations. This**
342 **structural arrangement suggests that F would be easily and almost totally released when the films are put in**
343 **contact with any food or culture media, where it can be solved, thus promoting the antimicrobial activity.**

344



345 **Figure 4** FESEM images of ferulic acid incorporated on the surface of PLA films using 96% ethanol
 346 solutions through adsorption (left) or pulverisation (right), at 100X and 400X. In the third row the film cross
 347 section is shown, exhibiting the F crystals on the top surface. The scale bars correspond to 100, 20 and 10
 348 µm for first, second and third rows respectively.

349

350 3.4. Electrospun PLA-Ferulic acid materials

351 The most relevant properties of the PLA-F solutions (density, electrical conductivity, viscosity and surface
 352 tension) affecting the electrospinning process (both regarding its feasibility and the final structure of the
 353 electrospun materials) were analysed and are shown in Table 2, along with the different solvent systems
 354 used. The density of all the solutions was close to 1 g/cm³, and Newtonian behaviour was found in every
 355 case with relatively small differences in viscosity. A1 was the densest and most viscous solution. Density,
 356 viscosity and surface tension were reduced when the proportion of ethyl acetate rose in the solvent systems,
 357 in coherence with the properties of the pure solvents (Smallwood, 1996). The solvent mixtures containing
 358 DMSO exhibited significantly higher values of electrical conductivity due to the higher value of the relative
 359 dielectric constant of DMSO ($\epsilon=46$), as compared to those of ethyl acetate and acetic acid (ϵ about 6)

(Smallwood, 1996). The morphology of the electrospun material is greatly affected by the properties of the solution, such as its viscosity, surface tension, electrical conductivity and surface charge density, as well as by the processing parameters (voltage, flow rate and collector distance) (Li & Wang, 2013). For low viscosity solutions, the surface tension is the controlling factor which determines whether beads or beaded fibres are formed (Shastri et al., 2009). By reducing the surface tension, for a determined concentration of the solution, beaded fibres can be converted into smooth fibres. Likewise, an increase in the electrical conductivity of the solution favours the formation of thinner fibres thus increasing the surface-to-volume ratio of the formed structures (Agrahari et al., 2017; Garg & Bowlin, 2011). Given that the electrical conductivity is the property with the highest differences between the studied solutions, it could be the factor determining the morphological differences between the electrospun samples.

Table 2. Properties of the PLA-F solutions (15 g PLA /100 g solution, 15 g F / 100 g solids) used in electrospinning processes with different solvents systems: ethyl acetate (E), DMSO (D) and glacial acetic acid (A) at different volumetric proportions.

Solution	Density (g/cm ³)	Conductivity (μS/cm)	Surface tension (mN/m)	Viscosity (Pa·s)
ED1:1	1.046±0.001 ^c	3.08±0.08 ^c	31.0±1.4 ^c	0.982±0.004 ^c
ED3:2	1.027±0.001 ^b	2.60±0.09 ^b	28.2±0.8 ^b	0.840±0.030 ^b
EA1:1	1.020±0.002 ^a	0.07±0.01 ^a	25.2±0.3 ^a	0.723±0.019 ^a
A1	1.085±0.002 ^d	0.08±0.01 ^a	25.0±0.4 ^a	1.263±0.016 ^d

Different superscripts ^{abc} indicate significant differences (p<0.05)

Successful operating conditions were obtained for the four solvent combinations (**Table 3**). The initial values of these operating conditions were based on previous studies into PLA using similar solvent systems (Tampau et al., 2020), and were empirically adjusted until a stable Taylor cone was observed. The solvents containing acetic acid (A) required a slightly lower voltage, and a stable Taylor cone could only be achieved at shorter distances to the collector. For the EA 1:1 solvent, the volumetric flow had to be increased. The process time was adjusted to prepare the samples destined for microbiological testing. The purpose was to obtain mats which were thick enough to reach the same target concentration of F in the sample (about 0.45 mg/cm²), which would imply about 1.1 mg of ferulic acid /mL of culture medium, when put in contact with the culture plate in the antimicrobial assays, assuming a total release.

Table 3. The electrospinning operation parameters and morphological dimensions of the nanomaterials obtained using different PLA and ferulic acid polymeric solutions (15 g PLA / 100 g solution, 15 g F / 100 g solids) with different solvents: ethyl acetate (E), DMSO (D) and acetic acid (A) in different volumetric proportions.

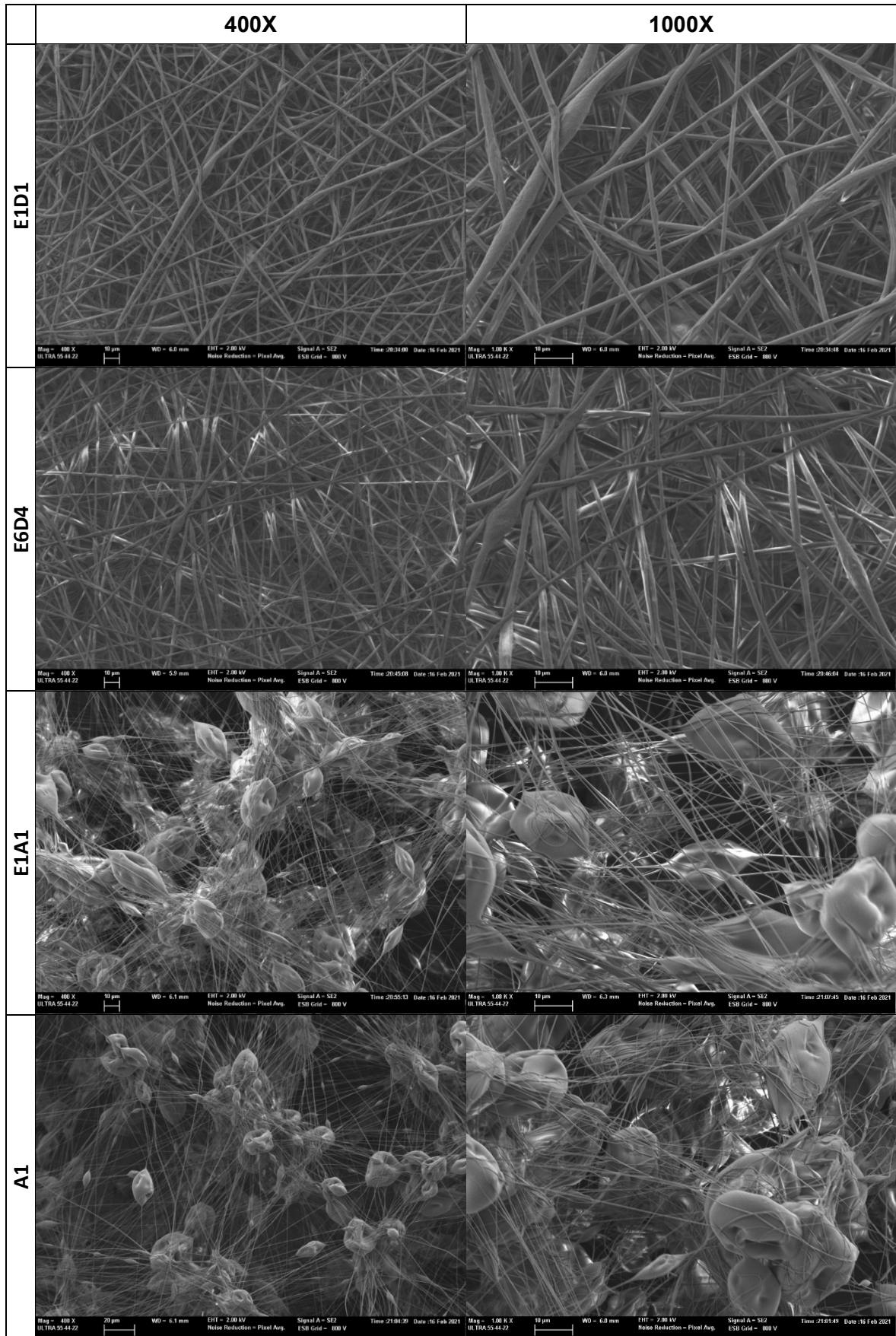
Formulation	Electrospinning operation parameters				Nanomaterial dimensions	
	Flow rate (μL/h)	Collector distance (cm)	Processing time (min)	Voltage (KV)	Fibre diameter (μm)	Bead diameter (μm)
ED1:1	1250	20	150	12-14	2,00±0,90 ^c	-
ED3:2	1250	20	150	12-14	1,50±0,30 ^b	-
EA1:1	2500	15	75	10-13	0,60±0,16 ^a	25±6 ^b
A1	1250	15	150	10-13	0,44±0,15 ^a	19±5 ^a

Different superscripts ^{abc} indicate significant differences (p<0.05)

Significant structural differences of the electrospun materials could be appreciated at a macroscopic scale. Solvent systems containing DMSO (ED1:1 and ED3:2) gave rise to fibrous mats, while those with acetic acid (EA1:1 and A1) yielded an electro-sprayed powdered layer, which was corroborated by FESEM analyses (**Figure 5**). **Table 3** shows the results of image analysis in order to quantify the characteristic diameters of fibres and beads. As can be observed, solvent mixtures with DMSO (ED1:1 and ED3:2) produced continuous nano-fibre structures, whose diameter was reduced when the DMSO content decreased in the solvent mixture. On the other hand, the structure of the samples produced with acetic acid mixtures (EA1:1 and A1) consists of beads connected with thinner fibres, where most of the material is concentrated in the beads.

396 When pure acetic acid was used, the diameters of both beads and fibres were smaller than those obtained
397 in the EA1:1 solvent. These structural differences **may be related to** the differences between the **electrical**
398 conductivity of the formulations. The greater conductivity of the systems with DMSO would give rise to a
399 higher acceleration of the stream and the maintenance of a continuous flow before reaching the collector
400 plate (Agrahari et al., 2017), **thus promoting fibre formation**.

401



402 **Figure 5** FESEM images of electrospun PLA nanomaterials containing ferulic acid, at 400X and 1000X
403 magnification levels (bars correspond to 20 and 10 µm, respectively), obtained with the different solvent
404 systems.

405

406 **3.5. Ferulic acid content in the materials obtained**

407 The F content of the different materials determined by methanolic extraction and **spectrophotometric**
 408 **quantification** is shown in **Table 4**, expressed as g of F per 100 g of material. The encapsulation efficiency
 409 **(mass of F quantified in the material with respect to the nominally incorporated, in percentage)** was also
 410 shown in **Table 4**. All the cast films exhibited high encapsulation efficiency (97%-100%) while the lowest
 411 value was obtained for some electrospun materials (84%-86%), which indicates that a small proportion of
 412 the initially incorporated F could be oxidised during the electrospinning process. Nevertheless, electrospun
 413 materials had the highest F content per gram of material, close to the amount incorporated into the solution
 414 (15% of total solids). In the case of the superficial incorporation of F, the pulverisation procedure proved to
 415 be more efficient than adsorption. This was due not only to the fact that more F was incorporated with lower
 416 solvent and time requirements, but also to the lack of film deformation that occurred during immersion in the
 417 adsorption process. Nevertheless, the different distribution of F in the different samples (inside the PLA
 418 matrix in cast films or electrospun mats and on the film surface in samples prepared by adsorption or
 419 pulverisation) could imply a variation in the antimicrobial activity of the films, depending on the amount of
 420 active released into the inoculated culture medium. Table 5 shows the estimated theoretical concentration
 421 **of F that would be** reached in the culture medium, assuming its complete release from the **PLA matrices**
 422 **coating the plates**. A wide range of theoretical concentrations can be seen, the electrospun samples
 423 providing the media with the lowest concentration, due to their lower thickness. Nevertheless, the real
 424 amount of active released in each case would be related with the antibacterial effect observed in the *in vitro*
 425 test.

426 **Table 4** Ferulic acid content in the different PLA materials, encapsulation efficiency (% ratio with respect to
 427 that nominally incorporated), theoretical F concentration (TFC) in the culture medium, assuming a
 428 complete release from the different PLA materials, and growth inhibition of *L. innocua*, with respect to the
 429 uncovered control samples, obtained in the *in vitro* tests with the different PLA materials.

Formulation	F content (% w/w)	Encapsulation efficiency (%)	TFC (mg/mL)	Growth inhibition (Log CFU/mL)
Casting - F2	1.96±0.04 ^a	97.0±2.0 ^a	1.05	0.01±0.02 ^a
Casting - F3	3.00±0.02 ^b	99.9±1.0 ^a	1.58	0.07±0.05 ^a
Casting - F5	4.90±0.11 ^c	98.2±2.2 ^a	2.63	0.01±0.07 ^a
Casting - F10	9.80±0.30 ^e	97.9±2.8 ^a	5.26	0.25±0.79 ^a
Adsorption	6.4±1.0 ^d	-	2.49	4.30±0.31 ^c
Pulverisation	10.0±1.5 ^e	-	3.87	4.11±0.42 ^c
ES-ED1:1	14.4±1.2 ^g	96±7 ^a	1.02	2.99±0.81 ^b
ES-ED3:2	12.9±0.7 ^f	86±5 ^b	0.92	3.26±0.33 ^b
ES-EA1:1	12.6±0.5 ^f	84±3 ^b	0.90	0.05±0.04 ^a
ES-A1	12.9±0.3 ^f	86±2 ^b	0.92	0.03±0.06 ^a

430 Different superscripts ^{abc} indicate significant differences (p<0.05)

431 **3.6. Antimicrobial activity of the materials obtained**

432 **Figure 6** shows the bacterial counts for *L. innocua* obtained in the *in vitro* tests with the different F loaded
 433 PLA materials, while the different growth inhibition values for the different PLA samples, with respect to the
 434 uncoated plate, can be observed in **Table 4**. According to a previous study, the Minimum Inhibitory
 435 Concentration (MIC) of ferulic acid for *L. innocua* is 0.7 mg/mL (Ordoñez et al., 2021), which would be
 436 surpassed in all cases provided the release of the acid from the materials into the culture media is complete.
 437 However, only in four cases did the materials reach 2 Log CFU/mL growth inhibition and, hence, an efficient
 438 antibacterial activity (Requena et al., 2019): these were those obtained by F adsorption or pulverisation and
 439 electrospun materials obtained with DMSO solvent systems (**ED1:1** and **ED3:2**) that were fibre structured.
 440 Despite the high concentration of F that could be theoretically reached in the culture media with a total
 441 release of F from cast films (up to 5.26 mg/mL in the cast film with 10% F), no significant growth inhibition
 442 occurred for these materials. The ineffectiveness of these films against *L. innocua* revealed no release of
 443 ferulic acid from the films regardless of their concentration. This was also observed in a previous study with
 444 thermoprocessed PLA films incorporating ferulic and cinnamic acids (Ordoñez et al., 2022). The glassy state
 445 of the polymer and the lack of swelling and relaxation when in contact with the aqueous culture media limited
 446 the molecular mobility and diffusion of ferulic molecules through the film matrix and only the most superficial
 447 amount of the compound was released to exert its antimicrobial power.

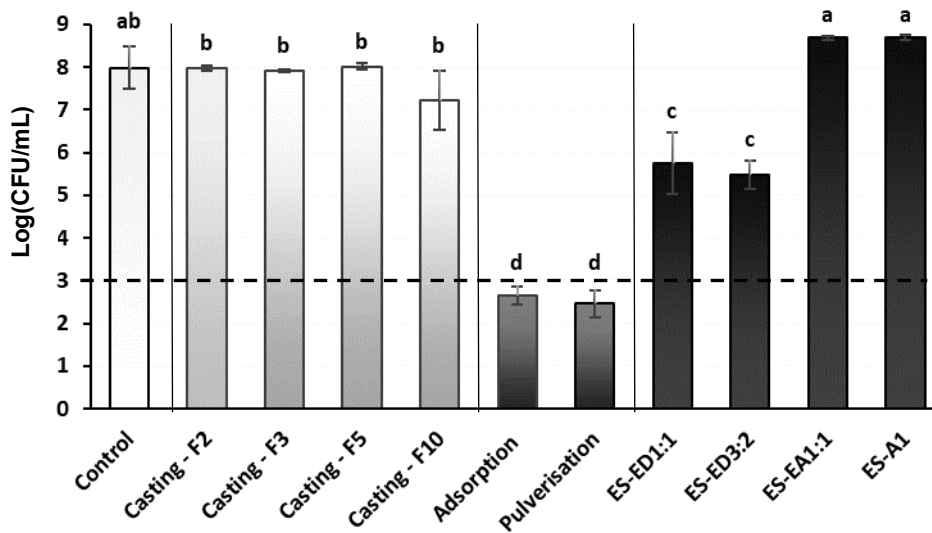
448 The active films obtained by the adsorption and pulverisation of F solutions, where the active compound was
 449 mainly incorporated onto the film surface, could easily release the active compound in contact with the

450 culture medium, thus being the most effective at inhibiting the growth of *L. innocua*. These films exhibited
451 similar antimicrobial power given the excess amount of F present on the film surface, thus easily releasing
452 the acid and provoking a bacteriostatic effect.

453 Electrospun materials contained about 14% ferulic acid. However, the plate-covering materials were very
454 thin, with just enough electrospun material to reach the MIC of ferulic acid on the plate, assuming a complete
455 release. The effectiveness of electrospun materials was dependent on their morphology. **Materials obtained**
456 **from DMSO mixture solutions**, having a fibre structure, exhibited a significant bacterial growth inhibition
457 whereas the mainly **bead-structured** mats showed no antibacterial effect. This could be explained by the
458 higher specific surface area of the fibres (Alonso-González et al., 2020) that can release the active
459 compound near the surface more effectively, reaching F concentration values closer to the MIC of bacteria
460 in the culture medium. In contrast, acetic acid-based materials with bead structures (**with lower**
461 **surface/volume ratio**) did not have enough ferulic acid near the surface to reach the MIC values and to inhibit
462 the bacterial growth.

463 The results obtained reveal that the release of ferulic acid is greatly hindered when **loaded** in PLA matrices,
464 the only possibility of enhancing the compound delivery being its surface retention. Therefore, it is the
465 location of the active compound in the material, and not its global concentration, that limits the obtaining of
466 antimicrobial materials with ferulic acid and PLA.

467



468 **Figure 6** *Listeria innocua* counts (mean value and standard deviation) after 6 days of incubation at 10 °C
469 for samples in contact with PLA-based materials loaded with ferulic acid (cast films with different content of
470 ferulic acid, thermoprocessed films surface-loaded with ferulic acid by adsorption or pulverisation, and
471 electrospun (ES) materials with the different solvents ED1:1, ED3:2, EA1:1 and A1). The control bar shows
472 mean growth for uncoated samples and the dotted line represents the initial inoculation.

473

474 Conclusions

475 Ferulic acid delivery from PLA matrices is greatly hindered due to the limited diffusion of the compound
476 through the matrix. Increase of ferulic loading did not provide the PLA matrices with compound delivery
477 capacity. Therefore, surface anchoring of the compound was the alternative method to obtain active PLA
478 materials with effective release of ferulic acid and antibacterial activity. This could be achieved by surface
479 adsorption from ferulic acid solutions or pulverisation of the solutions on the film surface. The adsorption
480 time and concentration of active compound in the solution must be fitted in order to obtain the target surface
481 concentration necessary to inhibit the bacterial growth, when delivered to the culture medium (or food).

482 Electrospun PLA materials loaded with ferulic acid can also be used as ferulic delivery systems, when the
483 process conditions and the properties of the solvent system promote fibre formation with high surface/volume
484 ratio. These fibres contain enough amount of the compound easily deliverable near the surface to reach the
485 minimal inhibitory concentration of the bacteria. These electrospun mats can be applied to obtain active food
486 packaging materials or others useful for biomedical applications, such as wound dressing or scaffolds for
487 neuronal tissue engineering, given the active properties of the compound.

488

489 **Acknowledgments**

490 The authors thank the Agencia Estatal de Investigación (Ministerio de Ciencia e Innovación, Spain) for the
491 financial support through projects AGL2016-76699-R and PID2019-105207RB-I00.

492 **Declaration of competing interest**

493 The authors declare that they have no known competing financial interests or personal relationships that
494 could have appeared to influence the work reported in this paper.

495 **CRedit authorship contribution statement**

496 **Ramón Ordoñez**: Investigation, Conceptualisation, Methodology, Formal analysis, Writing – original draft,
497 Writing – review & editing. **Lorena Atarés**: Conceptualisation, Methodology, Data curation, Writing – original
498 draft, Writing – review & editing, Supervision. **Amparo Chiralt**: Conceptualisation, Methodology, Data
499 curation, Writing – review & editing, Supervision, Project administration.

500 **References**

501

502 Agrahari, V., Agrahari, V., Meng, J., & Mitra, A. K. (2017). Electrospun Nanofibers in Drug
503 Delivery: Fabrication, Advances, and Biomedical Applications. *Emerging*
504 *Nanotechnologies for Diagnostics, Drug Delivery and Medical Devices*, 189–215.
505 <https://doi.org/10.1016/B978-0-323-42978-8.00009-7>

506 Alonso-González, M., Corral-González, A., Felix, M., Romero, A., & Martin-Alfonso, J. E. (2020).
507 Developing active poly(vinyl alcohol)-based membranes with encapsulated antimicrobial
508 enzymes via electrospinning for food packaging. *International Journal of Biological*
509 *Macromolecules*, 162, 913–921. <https://doi.org/10.1016/j.ijbiomac.2020.06.217>

510 Armentano, I., Bitinis, N., Fortunati, E., Mattioli, S., Rescignano, N., Verdejo, R., Lopez-
511 Manchado, M. A., & Kenny, J. M. (2013). Multifunctional nanostructured PLA materials
512 for packaging and tissue engineering. *Progress in Polymer Science*, 38(10–11), 1720–1747.
513 <https://doi.org/10.1016/j.progpolymsci.2013.05.010>

514 Atarés, L., & Chiralt, A. (2016). Essential oils as additives in biodegradable films and coatings
515 for active food packaging. *Trends in Food Science & Technology*, 48, 51–62.
516 <https://doi.org/10.1016/j.tifs.2015.12.001>

517 Bhattacharjee, P. K., & Rutledge, G. C. (2017). 5.12 Electrospinning and Polymer Nanofibers:
518 Process Fundamentals. In *Comprehensive Biomaterials II* (pp. 200–216). Elsevier.
519 <https://doi.org/10.1016/B978-0-08-100691-7.00165-8>

520 Castro Coelho, S., Nogueiro Estevinho, B., & Rocha, F. (2021). Encapsulation in food industry
521 with emerging electrohydrodynamic techniques: Electrospinning and electrospraying – A
522 review. *Food Chemistry*, 339(August 2020), 127850.
523 <https://doi.org/10.1016/j.foodchem.2020.127850>

524 Chen, H., Wang, C., Kang, H., Zhi, B., Haynes, C. L., Aburub, A., & Sun, C. C. (2020).
525 Microstructures and pharmaceutical properties of ferulic acid agglomerates prepared by
526 different spherical crystallization methods. *International Journal of Pharmaceutics*,
527 574(November 2019), 118914. <https://doi.org/10.1016/j.ijpharm.2019.118914>

528 Chung, J., & Kwak, S. (2019). Effect of nanoscale confinement on molecular mobility and drug
529 release properties of cellulose acetate/sulindac nanofibers. *Journal of Applied Polymer*
530 *Science*, 136(33), 47863. <https://doi.org/10.1002/app.47863>

- 531 Dávila-Guzman, N. E., Cerino-Córdova, F. J., Diaz-Flores, P. E., Rangel-Mendez, J. R., Sánchez-
532 González, M. N., & Soto-Regalado, E. (2012). Equilibrium and kinetic studies of ferulic acid
533 adsorption by Amberlite XAD-16. *Chemical Engineering Journal*, *183*, 112–116.
534 <https://doi.org/10.1016/j.cej.2011.12.037>
- 535 Garg, K., & Bowlin, G. L. (2011). Electrospinning jets and nanofibrous structures.
536 *Biomicrofluidics*, *5*(1), 013403. <https://doi.org/10.1063/1.3567097>
- 537 Itagaki, S., Kurokawa, T., Nakata, C., Saito, Y., Oikawa, S., Kobayashi, M., Hirano, T., & Iseki, K.
538 (2009). In vitro and in vivo antioxidant properties of ferulic acid: A comparative study
539 with other natural oxidation inhibitors. *Food Chemistry*, *114*(2), 466–471.
540 <https://doi.org/10.1016/j.foodchem.2008.09.073>
- 541 Jamshidian, M., Tehrani, E. A., & Desobry, S. (2012). Release of synthetic phenolic antioxidants
542 from extruded poly lactic acid (PLA) film. *Food Control*, *28*(2), 445–455.
543 <https://doi.org/10.1016/j.foodcont.2012.05.005>
- 544 Li, Z., & Wang, C. (2013). One-Dimensional nanostructures. In *Archives of Hellenic Medicine*
545 (Vol. 32, Issue 1). Springer Berlin Heidelberg. <https://doi.org/10.1007/978-3-642-36427-3>
- 546 Lorite, G. S., Rocha, J. M. R., Miilumäki, N., Saavalainen, P., Selkälä, T., Morales-Cid, G.,
547 Gonçalves, M. P., Pongrácz, E., Rocha, C. M. R., & Toth, G. (2017). Evaluation of
548 physicochemical/microbial properties and life cycle assessment (LCA) of PLA-based
549 nanocomposite active packaging. *LWT*, *75*, 305–315.
550 <https://doi.org/10.1016/j.lwt.2016.09.004>
- 551 Main, J. H., Clydesdale, F. M., & Francis, F. J. (1978). SPRAY DRYING ANTHOCYANIN
552 CONCENTRATES FOR USE AS FOOD COLORANTS. *Journal of Food Science*, *43*(6), 1693–
553 1694. <https://doi.org/10.1111/j.1365-2621.1978.tb07390.x>
- 554 Miyague, L., Macedo, R. E. F., Meca, G., Holley, R. A., & Luciano, F. B. (2015). Combination of
555 phenolic acids and essential oils against *Listeria monocytogenes*. *LWT - Food Science and*
556 *Technology*, *64*(1), 333–336. <https://doi.org/10.1016/j.lwt.2015.05.055>
- 557 Mota, F. L., Queimada, A. J., Pinho, S. P., & Macedo, E. A. (2008). Aqueous solubility of some
558 natural phenolic compounds. *Industrial and Engineering Chemistry Research*, *47*(15),
559 5182–5189. <https://doi.org/10.1021/ie071452o>
- 560 Muller, J., González-Martínez, C., & Chiralt, A. (2017a). Combination Of Poly(lactic) acid and
561 starch for biodegradable food packaging. *Materials*, *10*(8), 1–22.
562 <https://doi.org/10.3390/ma10080952>
- 563 Muller, J., Casado Quesada, A., González-Martínez, C., & Chiralt, A. (2017b). Antimicrobial
564 properties and release of cinnamaldehyde in bilayer films based on polylactic acid (PLA)
565 and starch. *European Polymer Journal*, *96*, 316–325.
566 <https://doi.org/10.1016/J.EURPOLYMJ.2017.09.009>
- 567 Ordoñez, R., Atarés, L., & Chiralt, A. (2021). Physicochemical and antimicrobial properties of
568 cassava starch films with ferulic or cinnamic acid. *LWT*, *144*(February), 111242.
569 <https://doi.org/10.1016/j.lwt.2021.111242>
- 570 Ordoñez, R., Atarés, L., & Chiralt, A. (2022). Effect of Ferulic and Cinnamic Acids on the
571 Functional and Antimicrobial Properties in Thermo-Processed Pla Films. *Food Packaging*
572 *and Shelf Life, Preprint*. <https://doi.org/10.2139/SSRN.3978978>
- 573 Paiva, L. B. de, Goldbeck, R., Santos, W. D. dos, & Squina, F. M. (2013). Ferulic acid and
574 derivatives: molecules with potential application in the pharmaceutical field. *Brazilian*

575 *Journal of Pharmaceutical Sciences*, 49(3), 395–411. <https://doi.org/10.1590/S1984->
576 82502013000300002

577 Peleg, M. (1988). An Empirical Model for the Description of Moisture Sorption Curves. *Journal*
578 *of Food Science*, 53(4), 1216–1217. <https://doi.org/10.1111/j.1365-2621.1988.tb13565.x>

579 Pernin, A., Bosc, V., Maillard, M.-N., & Dubois-Brissonnet, F. (2019). Ferulic Acid and Eugenol
580 Have Different Abilities to Maintain Their Inhibitory Activity Against *Listeria*
581 *monocytogenes* in Emulsified Systems. *Frontiers in Microbiology*, 10(FEB), 1–10.
582 <https://doi.org/10.3389/fmicb.2019.00137>

583 Pholosi, A., Naidoo, E. B., & Ofomaja, A. E. (2020). Intraparticle diffusion of Cr(VI) through
584 biomass and magnetite coated biomass: A comparative kinetic and diffusion study. *South*
585 *African Journal of Chemical Engineering*, 32(July 2019), 39–55.
586 <https://doi.org/10.1016/j.sajce.2020.01.005>

587 Requena, R., Vargas, M., & Chiralt, A. (2019). Eugenol and carvacrol migration from PHBV films
588 and antibacterial action in different food matrices. *Food Chemistry*, 277(October 2018),
589 38–45. <https://doi.org/10.1016/j.foodchem.2018.10.093>

590 Rice-Evans, C. A., Miller, N. J., & Paganga, G. (1996). Structure-antioxidant activity relationships
591 of flavonoids and phenolic acids. *Free Radical Biology and Medicine*, 20(7), 933–956.
592 [https://doi.org/10.1016/0891-5849\(95\)02227-9](https://doi.org/10.1016/0891-5849(95)02227-9)

593 Shakeel, F., Salem-Bekhit, M. M., Haq, N., & Siddiqui, N. A. (2017). Solubility and
594 thermodynamics of ferulic acid in different neat solvents: Measurement, correlation and
595 molecular interactions. *Journal of Molecular Liquids*, 236, 144–150.
596 <https://doi.org/10.1016/J.MOLLIQ.2017.04.014>

597 Shastri, V. P., Sy, J. C., & Klemm, A. S. (2009). Emulsion as a Means of Controlling
598 Electrospinning of Polymers. *Advanced Materials*, 21(18), 1814–1819.
599 <https://doi.org/10.1002/adma.200701630>

600 Shi, C., Zhang, X., Sun, Y., Yang, M., Song, K., Zheng, Z., Chen, Y., Liu, X., Jia, Z., Dong, R., Cui, L.,
601 & Xia, X. (2016). Antimicrobial Activity of Ferulic Acid Against *Cronobacter sakazakii* and
602 Possible Mechanism of Action. *Foodborne Pathogens and Disease*, 13(4), 196–204.
603 <https://doi.org/10.1089/fpd.2015.1992>

604 Smallwood, I. M. (1996). Handbook of Organic Solvent Properties. In *Handbook of Organic*
605 *Solvent Properties*. Elsevier. <https://doi.org/10.1016/C2009-0-23646-4>

606 Suhag, R., Kumar, N., Petkoska, A. T., & Upadhyay, A. (2020). Film formation and deposition
607 methods of edible coating on food products: A review. *Food Research International*, 136,
608 109582. <https://doi.org/10.1016/j.foodres.2020.109582>

609 Tampau, A., González-Martínez, C., & Chiralt, A. (2018). Release kinetics and antimicrobial
610 properties of carvacrol encapsulated in electrospun poly-(ϵ -caprolactone) nanofibres.
611 Application in starch multilayer films. *Food Hydrocolloids*, 79, 158–169.
612 <https://doi.org/10.1016/j.foodhyd.2017.12.021>

613 Tampau, A., González-Martínez, C., & Chiralt, A. (2020). Polylactic acid-based materials
614 encapsulating carvacrol obtained by solvent casting and electrospinning. *Journal of Food*
615 *Science*, 85(4), 1177–1185. <https://doi.org/10.1111/1750-3841.15094>

616 Wang, L., & Ryan, A. J. (2011). Introduction to electrospinning. *Electrospinning for Tissue*
617 *Regeneration*, 3–33. <https://doi.org/10.1533/9780857092915.1.3>

618 Zduńska, K., Dana, A., Kolodziejczak, A., & Rotsztein, H. (2018). Antioxidant Properties of
619 Ferulic Acid and Its Possible Application. *Skin Pharmacology and Physiology*, 31(6), 332–
620 336. <https://doi.org/10.1159/000491755>
621